# Suppression of $1/f^{\alpha}$ noise in one-qubit systems

Pekko Kuopanportti,[1,*] Mikko Möttönen,[1,2] Ville Bergholm,[1] Olli-Pentti Saira,[1,2] Jun Zhang,[3] and K. Birgitta Whaley[3]
[1]*Department of Engineering Physics–COMP, Helsinki University of Technology, P. O. Box 5100, 02015 TKK, Finland*
[2]*Low Temperatre Laboratory, Helsinki University of Technology, P. O. Box 5100, 02015 TKK, Finland*
[3]*Department of Chemistry and Pitzer Center for Theoretical Chemistry, University of California, Berkeley, California 94720, USA*
(Received 5 April 2007; published 20 March 2008)

We investigate the generation of quantum operations for one-qubit systems under classical Markovian noise with a $1/f^{\alpha}$ power spectrum, where $2>\alpha>0$. We present an efficient way to approximate the noise with a discrete multistate Markovian fluctuator. With this method, the average temporal evolution of the qubit state operator under $1/f^{\alpha}$ noise can be feasibly determined from recently derived deterministic master equations. We obtain qubit operations such as quantum memory and the NOT gate to high fidelity by a gradient-based optimization algorithm. For the NOT gate, the computed fidelities are qualitatively similar to those obtained earlier for random telegraph noise. In the case of quantum memory, however, we observe a nonmonotonic dependency of the fidelity on the operation time, yielding a natural access rate of the memory.

DOI: 10.1103/PhysRevA.77.032334 PACS number(s): 03.67.Pp, 03.65.Yz, 05.40.Ca

## I. INTRODUCTION

In solid-state realization of qubits, material-specific fluctuations typically induce the major contribution to the intrinsic noise. Much effort has been focused on the preservation of the state in a quantum memory in the presence of $1/f^{\alpha}$ noise, since this is a ubiquitous form of noise encountered in solid-state qubit applications such as charge and spin qubits [1–3]. Spin qubits such as those formed from donor electronic spins in semiconductors are susceptible to noise deriving from dipolar coupling to environmental nuclear spins. Recent work has shown that electron donor spins in silicon are subject to magnetic noise with a $1/f^{\alpha}$ spectrum that derives from relaxation of dangling bonds near oxygen vacancies at the $Si/SiO_2$ interface and that constitutes the dominant mechanism for phase fluctuations of donor spins near the surface [4]. Magnetic noise from electrons in defect states has also been postulated to be a contributing factor to $1/f^{\alpha}$ noise in superconducting devices [5,6]. Calculations for a phosphorus donor in silicon show that the high-frequency component of the nuclear spin noise on such donors in bulk is also approximately described by a $1/f^{\alpha}$ power spectrum, although non-Markovian contributions can render this more complex in certain configurations [7]. Closely related to $1/f^{\alpha}$ noise is random telegraph noise (RTN), which arises from the coupling of an individual bistable fluctuator to a qubit [2,8–14]. Superposition of multiple RTN sources is one well-known mechanism for the generation of a $1/f^{\alpha}$ noise spectrum [15–18]. The current work focuses on the suppression of qubit dephasing due to $1/f^{\alpha}$ noise under conditions of weak Markovian coupling of the qubit to its environment, conditions that are well met by the magnetic noise encountered by donor spins in semiconductors. We note that $1/f^{\alpha}$ noise is also frequently encountered in Josephson devices, with measurements of both charge [19,20] and critical current noise [21,22] showing $1/f^{\alpha}$ power spectral densities. Background charge fluctuations resulting in $1/f^{\alpha}$ noise spectra have been identified as responsible for low-frequency noise in single-electron transistors [23] and are also considered to be the most important source of dephasing in Josephson charge qubits [19,20,24]. However, noise in these systems can be dominated by strongly coupled and possibly non-Markovian fluctuators. In this case, they are not directly addressable with the methods we present here.

Several approaches to suppress decoherence based on pulse design have been proposed in the literature [25–30]. Dynamical decoupling schemes average out the unwanted effects of the environmental interaction through the application of suitable control pulses [27,28]. Application of these schemes often involves hard pulses with instantaneous switchings and unbounded control amplitudes, resulting in a limited range of validity. Nevertheless, dynamical decoupling with soft pulses slower than the fastest bath time scale were recently also shown to reduce the decoherence for $1/f^{\alpha}$ noise [29]. In Ref. [30], a direct pulse optimization method restricted to bounded control pulses was developed for implementing one-qubit operations in a noisy environment. That initial work on noise suppression addressed the example of a one-qubit system under the influence of classically modeled RTN, such as might arise from a single bistable fluctuator, and allowed mitigation of decoherence deriving from Markovian baths with arbitrary noise correlation time.

In this paper, we extend the work of Ref. [30] to suppress $1/f^{\alpha}$ noise where $2>\alpha>0$, in the Markovian setting. We investigate two ways to approximate the $1/f^{\alpha}$ noise for computer simulations, namely, the sum of independent RTN fluctuators and a single discrete multistate Markovian noise source. We show that the single fluctuator provides a much more efficient way to model $1/f^{\alpha}$ noise than independent RTN fluctuators. Furthermore, the average temporal evolution of the state operator under this Markovian noise can be exactly described by a set of deterministic master equations derived in Ref. [31]. Using this approach, we avoid the heavy computational task arising from the numerical evaluation of the state operator averaged over a large number of different sample paths of the noise as computed in Ref. [30]. This framework will not only significantly accelerate the

*pekko.kuopanportti@tkk.fi

 

convergence of the control pulse sequence optimization, but also allows further theoretical analysis. Using these master equations, we employ gradient-based optimization procedures to obtain pulse sequences that suppress $1/f^{\alpha}$ noise for quantum memory and for a NOT gate. Comparisons with composite pulses designed to eliminate systematic errors and with refocusing pulses demonstrate that the numerically optimized pulse sequences yield the highest fidelities. This method will be applicable to weakly coupled, Markovian noise sources with corresponding power spectra.

The remainder of this paper is organized as follows. In Sec. II, we show how to efficiently approximate $1/f^{\alpha}$ noise in a Markovian setting by a multistate Markovian fluctuator. In Sec. III, we define the fidelity of qubit operations, review the master equations describing the average evolution of the qubit state operator in the presence of the noise, and describe the numerial optimization procedure. Sections IV and V present optimized control pulse sequences and the achieved fidelities for quantum memory and for the NOT gate, respectively. Finally, Sec. VI concludes and indicates further applications of the method.

## II. ONE-QUBIT SYSTEM SUBJECT TO $1/f^{\alpha}$ NOISE

We consider a one-qubit system described by the effective Hamiltonian

$$H = \frac{1}{2}a(t)\sigma_x + \frac{1}{2}\eta(t)\sigma_z, \tag{1}$$

where $a(t) \in [-a_{\max}, a_{\max}]$ is the external control field applied along the $x$ direction and $\eta(t)$ is the classical noise signal perturbing the system along the $z$ direction. Since in real physical systems there is in general a maximum achievable coupling between the physical qubit and the external control fields, this implies that the control field must be bounded. The noise source $\eta(t)$ can be characterized by its autocorrelation function

$$C(t) \equiv \langle \eta(0)\eta(t)\rangle = \lim_{T\to\infty}\frac{1}{T}\int_{-T/2}^{T/2}\eta(s)\eta(s+t)ds, \tag{2}$$

the Fourier transformation of which defines the noise power spectral density as

$$S(f) = \int_{-\infty}^{\infty} C(t)e^{-i2\pi ft}dt. \tag{3}$$

For a single RTN source with the amplitude $\Delta$ and correlation time $\tau_c$, the autocorrelation function is given by [32]

$$C_{\mathrm{RTN}}(t) = \Delta^2 e^{-2|t|/\tau_c}, \tag{4}$$

and the corresponding power spectral density by

$$S_{\mathrm{RTN}}(f) = \frac{\Delta^2\tau_c}{1+(\pi f\tau_c)^2}. \tag{5}$$

A standard way to simulate $1/f^{\alpha}$ noise is to use an ensemble of $K$ independent, uncorrelated RTN processes [1,15,17]. Let $\eta_k(t)$ be a symmetric RTN signal switching between values $-\Delta_k$ and $\Delta_k$ with the correlation time $\tau_k$ and a corresponding transition rate $\gamma_k \equiv 1/\tau_k$. The total noise process appears in the Hamiltonian (1) as $\eta(t) = \Sigma_{k=1}^{K}\eta_k(t)$. Since the RTN sources are independent, Eqs. (2) and (4) yield the autocorrelation function

$$C(t) = \sum_{k=1}^{K}\Delta_k^2 e^{-2|t|/\tau_k} = \sum_{k=1}^{K}\Delta_k^2 e^{-2\gamma_k|t|}, \tag{6}$$

and the corresponding power spectral density is given by

$$S(f) = \sum_{k=1}^{K}\frac{\Delta_k^2\gamma_k}{\gamma_k^2+(\pi f)^2}. \tag{7}$$

Introducing the density of transition rates $g(\gamma)$ and expressing the noise strength $\Delta$ as a function of the transition rate, we can replace the summation in Eq. (7) by an integration, which yields

$$S(f) = \int_{\gamma_{\min}}^{\gamma_{\max}}\frac{\Delta^2(\gamma)g(\gamma)\gamma}{\gamma^2+(\pi f)^2}\mathrm{d}\gamma, \tag{8}$$

where $\gamma_{\min}$ and $\gamma_{\max}$ are the minimum and maximum transition rates in the ensemble, respectively. Provided that

$$\Delta^2(\gamma)g(\gamma) = 2A/\gamma, \tag{9}$$

where $A$ is a constant, the power spectral density in Eq. (8) becomes [17]

$$S(f) = \frac{2A}{\pi f}\left[\arctan\left(\frac{\gamma_{\max}}{\pi f}\right) - \arctan\left(\frac{\gamma_{\min}}{\pi f}\right)\right] \simeq \frac{A}{f},$$

$$\gamma_{\min} \ll \pi f \ll \gamma_{\max}. \tag{10}$$

Thus Eq. (10) yields an approximation to the $1/f$ power spectrum. To generate a general $1/f^{\alpha}$ power spectral density for $2 > \alpha > 0$, we can choose

$$\Delta^2(\gamma)g(\gamma) = 2A\gamma^{-\alpha} \tag{11}$$

as shown in [17].

Although the above method yields a valid approximation for the $1/f^{\alpha}$ spectrum, it is computationally inefficient. In particular, the number of distinct noise states increases exponentially with the number of RTN fluctuators, $K$, i.e., the number of terms in the sum of Eq. (7) approximating the $1/f^{\alpha}$ noise. Since the size of the differential equation system describing the average qubit dynamics increases linearly with the number of noise states [31], in practice one has to restrict the computation to a rather small number of independent RTN fluctuators.

To overcome this problem, we present a conceptually different way of generating the desired $1/f^{\alpha}$ noise spectrum using a single multistate Markovian fluctuator. Consider a continuous-time Markovian noise process with $M$ discrete noise states. Let $\Gamma_{kj}$ denote the transition rate from the $j$th to the $k$th state. In order to preserve total probability, we must have

$$\sum_{k=1}^{M} \Gamma_{kj} = 0 \quad \text{for all } j = 1,2,\ldots,M. \tag{12}$$

Let us assume that the transition rates are symmetric, i.e., $\Gamma = \Gamma^T$. Under this assumption the noise process has a steady-state solution in which the different noise states are equally probable. In order for the noise to be unbiased, i.e., $\langle \eta \rangle = 0$, the amplitudes $b_k$ associated with the noise states must satisfy

$$\sum_{k=1}^{M} b_k = 0. \tag{13}$$

The autocorrelation of this noise process is given by

$$C(t) = \langle \eta(t)\, \eta(0) \rangle = \frac{1}{M} b^T e^{\Gamma |t|} b. \tag{14}$$

Since $\Gamma$ is symmetric, we can diagonalize it with an orthogonal matrix $V$ as $\Gamma = V \Lambda V^T$, where the real diagonal matrix $\Lambda = \mathrm{diag}\{\lambda_k\}_{k=1}^{M}$ carries the eigenvalues of $\Gamma$ in a descending order. Defining $\chi := \frac{1}{\sqrt{M}} V^T b$, we may rewrite Eq. (14) in the form of Eq. (6) as

$$C(t) = \chi^T e^{\Lambda |t|} \chi = \sum_{k=1}^{M} \chi_k^2 e^{\lambda_k |t|}. \tag{15}$$

In order to use this multistate Markovian fluctuator to approximate $1/f^{\alpha}$ noise, we have to choose the eigenvalues $\lambda_k$ and the coefficients $\chi_k$ such that Eq. (11) is satisfied. Moreover, we must construct the orthogonal matrix $V$ such that $\Gamma = V \Lambda V^T$ satisfies Eq. (12), the amplitudes $b_k$ satisfy Eq. (13), and the off-diagonal elements of $\Gamma$ are non-negative. If this can be accomplished, we have provided an efficient way to implement $1/f^{\alpha}$ noise. Note that the $M$-state Markovian fluctuator, Eq. (15), corresponds formally to Eq. (6) with $M-1$ nonvanishing RTN fluctuators, which gives an exponential improvement in the efficiency of the noise approximation.

One way to satisfy the above requirements is to pick an integer $m \geq 2$, set $M = 2^m$, and choose the eigenvalues as

$$\{\lambda_k\}_{k=1}^{M} = -2\{0, \gamma_{\min}, \gamma_{\min} + \delta, \gamma_{\min} + 2\delta, \ldots, \gamma_{\max}\},$$

where $\gamma_{\max} = (M-2)\delta + \gamma_{\min}$ and $0 < \delta \leq \gamma_{\min}$. Hence the distribution of the transition rates $g(\gamma)$ is uniform on $[\gamma_{\min}, \gamma_{\max}]$. Then we set $V = \tilde{H}^{\otimes m}$, where $\tilde{H}$ is the Hadamard matrix

$$\tilde{H} = \frac{1}{\sqrt{2}} \begin{pmatrix} 1 & 1 \\ 1 & -1 \end{pmatrix}.$$

Explicit calculation shows that these conditions ensure that Eq. (12) is satisfied. To fulfill the conditions given by Eqs. (11) and (13), we set $\chi_1 = 0$ and $\chi_k = \gamma_k^{-\alpha/2}$ for $k = 2,\ldots,M$, where $\gamma_k$ is equal to $\gamma_{\min} + (k-2)\delta$. It can be shown that this construction will also produce transition matrices $\Gamma$ with non-negative off-diagonal elements.

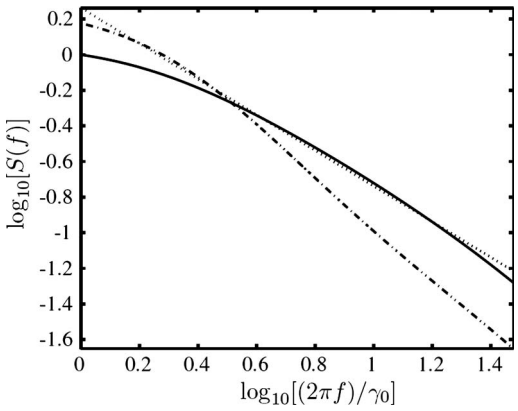


FIG. 1. Logarithm of the power spectral density for five independent RTN fluctuators (dash-dotted line), a multistate Markovian source corresponding to 31 RTN fluctuators (solid line), and an ideal $1/f$ noise (dotted line). The transition rates of the RTN fluctuators are in both cases distributed uniformly on the interval $[\gamma_0, 30\gamma_0]$.

Alternatively, we could choose the eigenvalues of $\Gamma$ in some other fashion and obtain a valid $V$ matrix using numerical optimization. This might result in an even more faithful approximation of $1/f^{\alpha}$ noise.

Figure 1 compares the approximation of the spectral density of $1/f$ noise generated by independent RTN sources and by a multistate Markovian source. For the RTN approach, we use five independent noise sources, for which the transition rates $\gamma_k$ are uniformly distributed in the range $[\gamma_{\min}, \gamma_{\max}] = [\gamma_0, 30\gamma_0]$, corresponding to correlation times varying non-uniformly from $\tau_c = 1/(30\gamma_0)$ to $\tau_c = 1/\gamma_0$, and for which the strengths are given by $\Delta_k = 1/\sqrt{\gamma_k}$. This corresponds to 32 distinct noise states. For the multistate fluctuator we use a 32-state noise source, the nonzero eigenvalues $\lambda_k$ of whose transition rate matrix $\Gamma$ are distributed uniformly on $[-30\gamma_0, -\gamma_0]$, and $\chi_k = 1/\sqrt{-\lambda_k}$. Thus the condition in Eq. (9) is satisfied for both of the approaches and the multistate noise source has an autocorrelation function and a power spectral density which are equal to those of a certain ensemble of 31 RTN fluctuators. We employ representations of similar computational complexity here in order to be able to assess their relative accuracy for a given computational effort.

Figure 1 shows that an ensemble of five RTN processes is not an accurate model for $1/f$ noise, whereas a single 32-state Markovian noise source is quite accurate. The difference in the accuracy is simply due to the number of parameters available for the approximation. In Fig. 1, the frequency range over which the approximation is accurate is relatively short if one considers that the $1/f^{\alpha}$ noise detected in experimental applications often extends over several frequency decades, but this is simply a matter of choosing a wider range for the eigenvalues of the matrix $\Gamma$. In order to preserve the accuracy of the approximation, the number of noise states $M$ in the Markovian source must be correspondingly increased.

For the purpose of demonstrating the feasibility of the numerical optimization algorithm, in the rest of this paper we will continue to approximate $1/f^{\alpha}$ noise by a single Markov-

ian noise source with 32 levels, with transition rates distributed uniformly over the interval $[\gamma_0, 30\gamma_0]$. We shall compare different $1/f^\alpha$ noise sources using their longest correlation time scale $\tau_c \equiv 1/\gamma_0$ as a parameter, which we refer to as the characteristic correlation time. The strength of the noise is fixed to $\langle|\eta|\rangle = \frac{1}{32}\Sigma_k |b_k| = 0.125 a_{\max}$. Alternatively, we could use the root mean square scaling, given by $\sqrt{\langle \eta^2 \rangle} = \sqrt{\frac{1}{32}\Sigma_k b_k^2}$. However, with the construction we employ here, these are equivalent, i.e., $\langle|\eta|\rangle \approx 0.568\sqrt{\langle \eta^2 \rangle}$.

## III. QUBIT DYNAMICS AND CONTROL

In Ref. [30], the temporal evolution of the qubit state operator was calculated by averaging over $10^4$–$10^5$ unitary quantum trajectories, each corresponding to a sample noise path. To ensure accuracy, a large number of unitary trajectories are required, which results in an extensive computational effort. In Ref. [31], exact deterministic master equations describing the average temporal evolution of quantum systems under Markovian noise arising from a classical multistate noise source were derived. A similar analysis was made in Ref. [33] for a two-state noise source. As was shown in Ref. [31], these master equations imply the same average dynamics as that given by the corresponding unitary quantum trajectory approach [30]. In the weak coupling situation, i.e., when the Born approximation can be assumed, the master equations for classical noise were in fact shown to accurately model dynamics of system coupled to certain quantum baths. We note that a generalized set of master equations applicable in principle also to non-Markovian noise was presented in Ref. [25].

Following Ref. [31], we introduce a conditional state operator $\rho_k(t)$ which corresponds to the state operator of the system averaged over all the noise sample paths occupying the $k$th state at the time instant $t$. The conditional state operators are normalized such that the trace of the operator $\rho_k(t)$ yields the probability of the $k$th noise state as $P_k(t) = \mathrm{Tr}[\rho_k(t)]$. The total average state operator can be expressed as

$$\rho(t) = \sum_k \rho_k(t). \tag{16}$$

The dynamics of $\rho_k$ is obtained from the coupled master equations [31]

$$\partial_t \rho_k(t) = \frac{1}{i\hbar}[H_k(t), \rho_k(t)] + \sum_j \Gamma_{kj}\rho_j(t), \tag{17}$$

where $H_k(t)$ is the Hamiltonian of the system corresponding to the $k$th noise state, and $\Gamma_{kj}$ the transition rate from the $j$th to the $k$th state, as defined in Sec. II. Specifically, in our one-qubit case,

$$H_k(t) = \frac{1}{2}a(t)\sigma_x + \frac{1}{2}b_k\sigma_z, \tag{18}$$

where $b_k$ is the noise amplitude of the state $k$. We shall use $\mathcal{E}_a\{\rho\}$ to denote the state $\rho$ evolved under the influence of noise and the control sequence $a$.

The fidelity function quantifying the overlap between the desired state $\rho_f$ and the actual achieved final state is defined as

$$\phi(\rho_f, \mathcal{E}_a\{\rho_0\}) = \mathrm{Tr}[\rho_f^\dagger \mathcal{E}_a\{\rho_0\}], \tag{19}$$

where $\rho_0$ is the initial state of the system. To measure how close the evolution $\mathcal{E}_a$ is to the intended quantum gate operation $U$, we calculate the average of the fidelity $\phi(U\rho_0 U^\dagger, \mathcal{E}_a\{\rho_0\})$ over all pure initial states $\rho_0$, and obtain the gate fidelity function [30]

$$\Phi(U) = \frac{1}{2} + \frac{1}{12}\sum_{k=x,y,z} \mathrm{Tr}[U\sigma_k U^\dagger \mathcal{E}_a\{\sigma_k\}]. \tag{20}$$

We aim to find the optimal control pulses which maximize the fidelity of the achieved quantum operation, and hence apply a typical gradient-based optimization algorithm such as the gradient ascent pulse engineering (GRAPE) method developed in Ref. [34]. If the continuous pulse profiles are approximated by piecewise constant functions, the gradient of the fidelity function with respect to these constant pulse values and durations can be calculated by the chain rule. This gradient is further used as a proportional adjustment to update the control pulse profile. The optimization procedure is terminated when a certain desired accuracy is achieved. Note that, due to the nonconvex nature of the problem, the gradient-based algorithm will yield only a locally optimal solution. We therefore subsequently vary the initial conditions to find the control pulse that achieves the highest gate fidelity.

## IV. QUANTUM MEMORY

In this section, we focus on the implementation of quantum memory, i.e., the identity operator. For the purpose of comparison with the optimized pulse sequences, we introduce four other kinds of control schemes which generate the identity operator.

The first reference sequence is simply not to apply any external control pulse, i.e., $a(t)=0$. This pulse has no compensation for decoherence or error. The second reference sequence is a constant $2\pi$ pulse given by

$$a_{2\pi}(t) = a_{\max}, \quad \text{for } t \in [0, 2\pi\hbar/a_{\max}]. \tag{21}$$

The third reference sequence is the composite pulse sequence known as compensation for off-resonance with a pulse sequence (CORPSE), which was originally designed to correct systematic errors in the implementation of one-qubit quantum operations and to provide high-order control protocols for systematic qubit bias, i.e., for the noise characteristic correlation time $\tau_c \to \infty$ [35,36]. For the identity operation, the CORPSE pulse sequence can be obtained as

$$a_{\mathrm{SC}2\pi}(t) = \begin{cases} a_{\max} & \text{for } 0 < t' < \pi, \\ -a_{\max} & \text{for } \pi \le t' \le 3\pi, \\ a_{\max} & \text{for } 3\pi < t' < 4\pi, \end{cases} \tag{22}$$

where the dimensionless time $t'$ is defined as $t' = a_{\max} t/\hbar$.

In the absence of noise, the CORPSE sequence generates the identity operator exactly although it requires twice as

long an operation time as a $2\pi$ pulse, the second reference pulse above. In the presence of small systematic errors, the CORPSE sequence is much more accurate than the $2\pi$ pulse. For example, consider a state transformation from the north pole back to itself on the Bloch sphere. For $\eta(t) \equiv \Delta$ in Eq. (1), the fidelities defined in Eq. (19) can be derived to be

$$\phi_{2\pi} = 1 - \frac{\pi^2}{4}\left(\frac{\Delta}{a_{\max}}\right)^4 + O\left(\frac{\Delta}{a_{\max}}\right)^6 \tag{23}$$

and

$$\phi_{\mathrm{SC}2\pi} = 1 - 4\pi^2\left(\frac{\Delta}{a_{\max}}\right)^8 + O\left(\frac{\Delta}{a_{\max}}\right)^{10}. \tag{24}$$

We observe that the error in the fidelity of the $2\pi$ pulse is fourth order in the relative noise strength $\Delta/a_{\max}$, whereas for the CORPSE pulse sequence it is eighth order. Thus the CORPSE sequence is much more accurate than a $2\pi$ pulse in correcting the effects of systematic errors on quantum memory.

The fourth standard pulse sequence which we take as a reference is the Carr-Purcell-Meiboom-Gill (CPMG) [37] sequence which is designed to preserve qubit coherence. In our context, this sequence consists of a $\pi/2$ pulse followed by multiple $\pi$ pulses at intervals $t_p$, followed by a final $\pi/2$ pulse to bring the system back to the original state. This pulse sequence is designed for dephasing time measurements on spins, starting from the $|0\rangle$ state. Thus one does not expect a CPMG pulse sequence to perform as well if the initial state is averaged over the Bloch sphere, as is done to compute a gate fidelity.

We first present the fidelities obtained for the identity operator using the various control pulse options in the presence of $1/f$ noise. The noise model used here is the single Markovian noise source defined at the end of Sec. II. In Fig. 2, the fidelities obtained from optimized control pulses, $2\pi$ pulse, CORPSE, CPMG, and zero pulse sequences are plotted as functions of the characteristic correlation time $\tau_c$ of the approximate $1/f$ noise. Here, CPMG1 and CPMG2 refer to two CPMG types of pulses with the intervals between $\pi$ pulses being $\pi$ and $2\pi$, respectively. The total duration for these pulses are all $12\pi\hbar/a_{\max}$. The optimal control pulse is designed for $6\pi$, and therefore we repeat it twice. Similarly, we repeat the $2\pi$ pulse six times, the CORPSE sequence three times, the CPMG1 sequence three times, and the CPMG2 sequence twice. The optimal control pulse yields clearly the highest fidelity among all these pulses, whereas the zero pulse sequence has the worst performance as there are no correction mechanisms. Note that, due to motional narrowing, all curves approach unit fidelity in the limit $\tau_c \to 0$.

The memory access rate is an important specification in modern computer technology [38]. In our context, it corresponds to the total duration of the control pulses. Figure 3 shows the fidelity as a function of the duration for the numerically optimized control pulses. Equation (1) implies that, in the absence of noise, the quantum system will generate an identity operator for $a = a_{\max}$ and the duration $T = 2n\pi/a_{\max}$. In Fig. 3, we observe that, despite an overall decrease, there

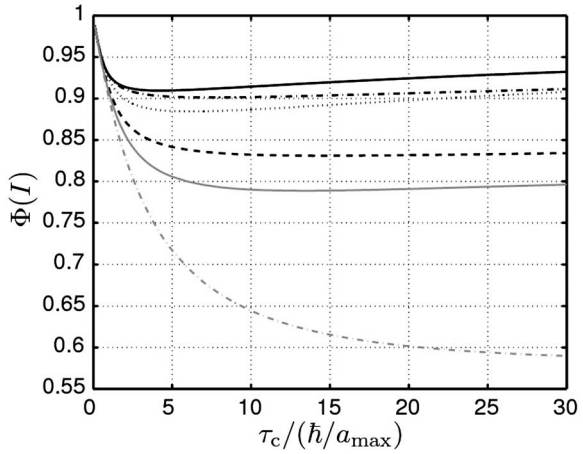


FIG. 2. Fidelity of the quantum memory as a function of the characteristic correlation time $\tau_c$ for optimized control pulses (black solid), a $2\pi$ pulse (black dash-dotted), CORPSE pulse sequence (black dotted), CPMG1 pulse sequence (black dashed), CPMG2 pulse sequence (gray solid), and zero pulse sequence (gray dash-dotted). The operation time is chosen to be $12\pi\hbar/a_{\max}$. The noise is produced using the multistate Markovian source defined at the end of Sec. II.

are peaks in the fidelity near these operation times. Thus we can regard $2n\pi/a_{\max}$ as the natural periods for quantum memory, and we always choose the total duration of control pulses correspondingly.

Figure 4 shows the fidelity of the quantum memory as a function of the noise strength $\langle|\eta|\rangle$ for the optimized control pulses, the $2\pi$ pulse, the CORPSE, CPMG1, CPMG2, and zero pulse sequences, using a fixed value for the characteristic correlation time $\tau_c = 30\hbar/a_{\max}$. At small values of $\langle|\eta|\rangle$ again, the optimized control pulses consistently achieve higher fidelities than all reference pulses. However, we note that if the noise strength exceeds $\sim 0.4$, the optimized pulse sequence reduces to the zero pulse sequence, i.e., any nonzero pulse sequence will actually deteriorate the fidelity performance.

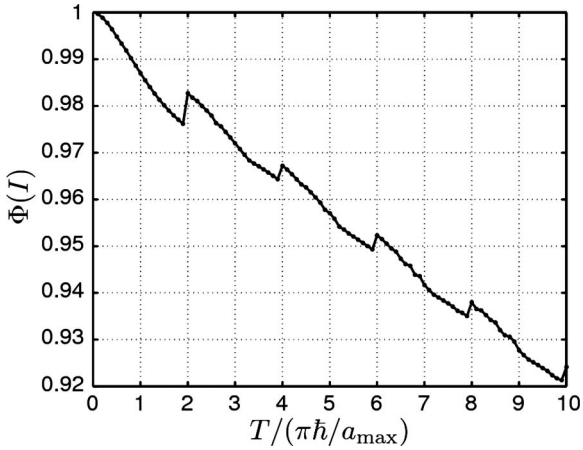


FIG. 3. Fidelity of the quantum memory as a function of the operation time for control pulses optimized at each point. The noise is produced by a similar multistate Markovian source as in Fig. 2, with characteristic correlation time $\tau_c = 3\hbar/a_{\max}$.

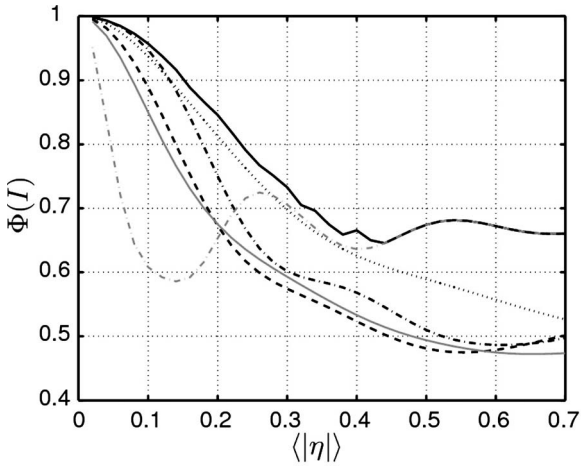


FIG. 4. Fidelity of the quantum memory as a function of the average absolute noise strength for optimized control pulses (black solid), $2\pi$ pulse (black dash-dotted), CORPSE (black dotted), CPMG1 (black dashed), CPMG2 (gray solid), and zero (gray dash-dotted). The operation time is chosen to be $12\pi\hbar/a_{\max}$. Except for its strength, the noise is produced by a similar multistate Markovian source as in Fig. 2 with the characteristic correlation time $\tau_c=30\hbar/a_{\max}$.

The discussion above is based on the specific noise density spectrum $1/f^{\alpha}$ with $\alpha=1$. Figure 5 shows the fidelities of quantum memory for four optimized control pulses, each of which is obtained for a different value of $\alpha$. The total duration of each control pulse is fixed to $6\pi$. A systematic scaling of the characteristic correlation time axis with respect to $\alpha$ is clearly visible in Fig. 5. This phenomenon is explained by the fact that the concentration of the power spectrum of $1/f^{\alpha}$ to low frequencies, i.e., long characteristic correlation times, increases with $\alpha$. Hence, the curves scale down in $\tau_c$ with increasing $\alpha$.

## V. NOT GATE

In this section, we focus on the generation of high-fidelity NOT gates, i.e., the $\sigma_x$ operator, under $1/f$ noise. As in the case of quantum memory, we compare the numerically optimized results with reference pulses. In this case, our first reference pulse is the $\pi$ pulse given by

$$a_{\pi}(t)=a_{\max} \quad \text{for} \quad t\in[0,\pi\hbar/a_{\max}], \tag{25}$$

which in the absence of noise is the most efficient way of achieving a NOT gate. In addition, we will use the two composite pulse sequences CORPSE and short CORPSE [35,36] which assume here the forms

$$a_{\mathrm{C}\pi}(t)=\begin{cases} a_{\max} & \text{for } 0<t'<\pi/3, \\ -a_{\max} & \text{for } \pi/3\le t'\le 2\pi, \\ a_{\max} & \text{for } 2\pi<t'<13\pi/3, \end{cases} \tag{26}$$

and

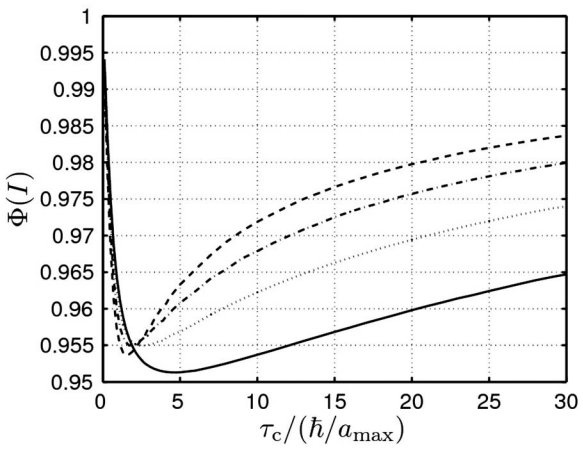


FIG. 5. Fidelity of the quantum memory achieved with optimized control pulses as a function of the characteristic correlation time $\tau_c$ for $1/f^{\alpha}$ noise with $\alpha=1$ (solid), 1.25 (dotted), 1.5 (dash-dotted), and 1.75 (dashed). The operation time is chosen to be $6\pi\hbar/a_{\max}$. The noise is produced by a similar multistate Markovian source as in Fig. 2 with variable values of the power $\alpha$.

$$a_{\mathrm{SC}\pi}(t)=\begin{cases} -a_{\max} & \text{for } 0<t'<\pi/3, \\ a_{\max} & \text{for } \pi/3\le t'\le 2\pi, \\ -a_{\max} & \text{for } 2\pi<t'<7\pi/3, \end{cases} \tag{27}$$

respectively. Both of these pulse sequences correct for systematic error, CORPSE being more efficient. However, the operation time of short CORPSE is much shorter than that of CORPSE, and hence it can yield higher fidelities in the presence of noise.

Figure 6 shows the NOT gate fidelities obtained by the reference and optimized pulses in the presence of the same $1/f$ noise as employed in the analysis of quantum memory in Sec. IV. We observe that, for long enough characteristic correlation times, the composite pulse sequences provide good error correction. Furthermore, as observed earlier for RTN

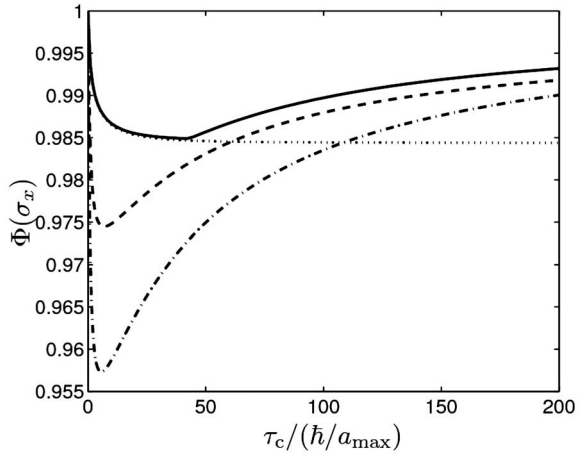


FIG. 6. NOT gate fidelities as functions of the characteristic noise correlation time $\tau_c$ for a $\pi$ pulse (dotted), CORPSE (dash-dotted), short CORPSE (dashed), and gradient optimized pulse sequence (solid). The $1/f$ noise is generated as in Fig. 2.

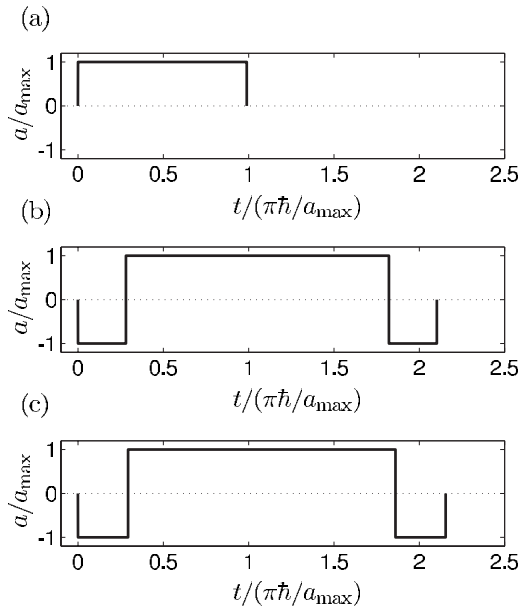


FIG. 7. Optimized pulse sequences yielding the highest gate fidelities for characteristic correlation times $\tau_c$ equal to (a) $45\hbar/a_{\max}$, (b) $100\hbar/a_{\max}$, and (c) $150\hbar/a_{\max}$, corresponding to Fig. 6.

[30], for intermediate characteristic correlation times, short CORPSE achieves the highest fidelity among the reference pulses. Figure 7 presents the pulse sequences obtained from the numerical optimizations for three different values of the noise characteristic correlation time $\tau_c$. For the optimized pulse sequence, we find a transition from an approximately constant pulse to a short-CORPSE-like pulse sequence at characteristic correlation time $\tau_c \approx 50\hbar/a_{\max}$. This change in optimal pulse sequence is responsible for the apparent discontinuity in the first derivative of the fidelity curve in Fig. 6.

These results for the generation of NOT gates under $1/f$ noise are qualitatively quite similar to the previous results presented in Refs. [30,31] for a single RTN. This similarity is due to the fact that $1/f$ noise can be regarded as arising from a sum of independent RTN fluctuators, each of which having a similar fidelity dependence on their correlation times. Note that the scale for the characteristic correlation time $\tau_c$ of the fidelity obtained in the presence of $1/f$ noise in Fig. 6 is somewhat different from the corresponding scale for the correlation time of a single RTN source, since the $1/f$ noise involves an ensemble of RTN fluctuators with a range of correlation times.

## VI. CONCLUSIONS

We have studied a single qubit under the influence of $1/f^{\alpha}$ noise for $2>\alpha>0$ and investigated how decoherence due to this noise can be suppressed in the implementation of single-qubit operations. We presented an efficient way to approximate the noise with a discrete multistate Markovian fluctuator. Due to this finding, the average temporal evolution of the qubit state operator under $1/f^{\alpha}$ noise can be efficiently determined from a deterministic master equation.

Employing these exact deterministic master equations describing the temporal evolution of the qubit state operator under Markovian noise, we applied a gradient-based optimization procedure to search for optimal control pulses implementing quantum operations. In particular, we studied the physical application of quantum memory, i.e., the identity operator, which is a fundamental concept in the realization of a quantum computer. The optimized control pulses significantly improved the fidelity over several reference pulse sequences such as the $2\pi$, CORPSE, and CPMG pulses. We observed peaks on fidelity curves corresponding to integer multiples of $2\pi\hbar/a_{\max}$ in the total durations of control pulses, where $a_{\max}$ is the maximum magnitude of the external control field. We also studied the performance of optimal control pulses under $1/f^{\alpha}$ noise for several different values of $2>\alpha\geq 1$, and found a monotonic behavior in the noise frequency as a function of $\alpha$, i.e., the fidelity curves are scaled down in the correlation time for increasing $\alpha$. We also investigated how the fidelities degraded as the noise strength increases. For the generation of high-fidelity NOT gates, we obtained results showing qualitatively similar behavior to the previous results presented in Refs. [30,31] for a single RTN source. In particular, just as for a single noise source, in the presence of $1/f^{\alpha}$ noise we observed a transition in the optimal control pulse sequence from a constant pulse to a CORPSE-like sequence as the noise characteristic correlation time $\tau_c$ is increased.

This approach of coupled master equations indexed by noise states of the environment together with an optimization technique for pulse design can be readily generalized to multiple qubits evolving in the presence of $1/f^{\alpha}$ noise and other Markovian noise sources. Hence it will be useful for protection of multiqubit gates as well as for stabilization of swapping of quantum information from a work qubit to long-term quantum memory. Furthermore, it can be used to develop realistic pulse sequences for mitigation of nuclear spin and surface magnetic noise acting on donor electron spins implanted in silicon [39] where the noise is considerably weaker than the examples studied in this work, as well as for suppression of background charge noise acting on superconducting qubits [19]. Applications to magnetic spin noise for dopants in silicon [4] and to protection of two-qubit gates in coupled qubit systems are under way. Further theoretical issues of interest include extending the approach to deal with multiple frequency decades of $1/f^{\alpha}$ noise and analysis of the dependence of the resulting pulse sequences on the noise amplitude distribution, as well as to non-Markovian noise sources.

## ACKNOWLEDGMENTS

This work was supported by the Academy of Finland, by the National Security Agency (NSA) under Grant No. MOD713106A, and by the NSF ITR program under Grant No. EIA-0205641. M.M. and V.B. acknowledge the Finnish Cultural Foundation and M.M. the Väisälä Foundation and Magnus Ehrnrooth Foundation for financial support. We thank J. Clarke, K. Young, and R. de Sousa for insightful discussions.

[1] L. Faoro and L. Viola, Phys. Rev. Lett. **92**, 117905 (2004).
[2] E. Paladino, L. Faoro, G. Falci, and R. Fazio, Phys. Rev. Lett. **88**, 228304 (2002).
[3] G. Falci, A. D'Arrigo, A. Mastellone, and E. Paladino, Phys. Rev. A **70**, 040101(R) (2004).
[4] R. de Sousa, Phys. Rev. B **76**, 245306 (2007).
[5] R. H. Koch, D. P. DiVincenzo, and J. Clarke, Phys. Rev. Lett. **98**, 267003 (2007).
[6] L. Faoro and L. Ioffe, e-print arXiv:0712.2834.
[7] R. de Sousa, e-print arXiv:cond-mat/0610716.
[8] Y. Nakamura, Y. A. Pashkin, T. Yamamoto, and J. S. Tsai, Phys. Rev. Lett. **88**, 047901 (2002).
[9] Y. M. Galperin, B. L. Altshuler, J. Bergli, and D. V. Shantsev, Phys. Rev. Lett. **96**, 097009 (2006).
[10] B. Savo, F. C. Wellstood, and J. Clarke, Appl. Phys. Lett. **50**, 1757 (1987).
[11] R. T. Wakai and D. J. Van Harlingen, Phys. Rev. Lett. **58**, 1687 (1987).
[12] T. Fujisawa and Y. Hirayama, Appl. Phys. Lett. **77**, 543 (2000).
[13] C. Kurdak, C.-J. Chen, D. C. Tsui, S. Parihar, S. Lyon, and G. W. Weimann, Phys. Rev. B **56**, 9813 (1997).
[14] R. de Sousa, K. B. Whaley, F. K. Wilhelm, and J. von Delft, Phys. Rev. Lett. **95**, 247006 (2005).
[15] M. B. Weissman, Rev. Mod. Phys. **60**, 537 (1988).
[16] E. Paladino, L. Faoro, G. Falci, and R. Fazio, Phys. Rev. Lett. **88**, 228304 (2002).
[17] B. Kaulakys, V. Gontis, and M. Alaburda, Phys. Rev. E **71**, 051105 (2005).
[18] Y. M. Galperin, B. L. Altshuler, J. Bergli, and D. V. Shantsev, Phys. Rev. Lett. **96**, 097009 (2006).
[19] O. Astafiev, Y. A. Pashkin, Y. Nakamura, T. Yamamoto, and J. S. Tsai, Phys. Rev. Lett. **96**, 137001 (2006).
[20] O. Astafiev, Y. A. Pashkin, Y. Nakamura, T. Yamamoto, and J. S. Tsai, Phys. Rev. Lett. **93**, 267007 (2004).
[21] F. C. Wellstood, C. Urbina, and J. Clarke, Appl. Phys. Lett. **85**, 5296 (2004).
[22] M. Mück, M. Korn, C. G. A. Mugford, J. B. Kycia, and J. Clarke, Appl. Phys. Lett. **86**, 012610 (2005).
[23] G. Zimmerli, T. M. Eiles, R. L. Kautz, and J. M. Martinis, Appl. Phys. Lett. **61**, 237 (1992).
[24] Y. Nakamura, Y. A. Pashkin, T. Yamamoto, and J. S. Tsai, Phys. Scr. T **102**, 155 (2002).
[25] A. G. Kofman and G. Kurizki, Phys. Rev. Lett. **87**, 270405 (2001).
[26] A. G. Kofman and G. Kurizki, Phys. Rev. Lett. **93**, 130406 (2004).
[27] L. Viola and S. Lloyd, Phys. Rev. A **58**, 2733 (1998).
[28] L. Viola, S. Lloyd, and E. Knill, Phys. Rev. Lett. **83**, 4888 (1999).
[29] K. Shiokawa and D. A. Lidar, Phys. Rev. A **69**, 030302(R) (2004).
[30] M. Möttönen, R. de Sousa, J. Zhang, and K. B. Whaley, Phys. Rev. A **73**, 022332 (2006).
[31] O.-P. Saira, V. Bergholm, T. Ojanen, and M. Möttönen, Phys. Rev. A **75**, 012308 (2007).
[32] M. J. Kirton and M. J. Uren, Adv. Phys. **38**, 367 (1989).
[33] J. Ankerhold and P. Pechukas, Europhys. Lett. **52**, 264 (2000).
[34] N. Khaneja, T. Reiss, C. Kehlet, T. Schulte-Herbrüggen, and S. J. Glaser, J. Magn. Reson. **172**, 296 (2005).
[35] H. K. Cummins and J. A. Jones, New J. Phys. **2**, 6 (2000).
[36] H. K. Cummins, G. Llewellyn, and J. A. Jones, Phys. Rev. A **67**, 042308 (2003).
[37] S. Meiboom and D. Gill, Rev. Sci. Instrum. **29**, 688 (1958).
[38] J. L. Hennessy and D. A. Patterson, *Computer Architecture: A Quantitative Approach* (Morgan Kaufmann, San Francisco, 2006).
[39] T. Schenkel, J. A. Liddle, A. Persaud, A. M. Tyryshkin, S. A. Lyon, R. de Sousa, K. B. Whaley, J. B. J. Shangkuan, and I. Chakarov, Appl. Phys. Lett. **8**, 11201 (2006).